Sensitivity of cross sections to the diffuseness of the confining potential in time-dependent close-coupling calculations of the double photoionization of He@C_{60}

Teck-Ghee Lee,* J. A. Ludlow,† and M. S. Pindzola
Department of Physics, Auburn University, Auburn, Alabama 36849, USA
(Received 26 October 2012; published 28 January 2013)

Calculations of the photoionization of endofullerenes often use a square-well potential to represent the confining fullerene. The sensitivity of the photoionization cross sections to the form of this model potential is explored here by the use of a diffuse potential. The cross sections for single photoionization with excitation and double photoionization of He@C_{60} are found to show damping of the confinement resonance structure as the degree of diffuseness is increased using a commonly adopted well depth of 8.22 eV. For a deeper well depth of 11.00 eV, the double-photoionization cross section is found to be insensitive to the diffuseness of the confining potential, as has also been reported recently for the single photoionization of H@C_{60} and Xe@C_{60} [Dolmatov, King, and Oglesby, J. Phys. B **45**, 105102 (2012)].

DOI: 10.1103/PhysRevA.87.015401 PACS number(s): 32.80.Fb, 36.40.Vz

I. INTRODUCTION

The photoionization of endofullerenes is a subject of long-standing theoretical (for a recent overview of the field, see Ref. [1]) and increasing experimental interest [2]. Theoretical studies are faced with the challenge of accurately representing the fullerene cage, a complex multielectron system, in a computationally tractable way. The solutions adopted fall into two main categories. The first is the time-dependent local-density approximation (TDLDA) in which the atom and enclosing fullerene are treated using a density-functional-theory approach [3]. The second approach is the use of a model potential to approximate the fullerene with model parameters matched to experiment. The model potentials adopted have included a δ-function approximation [4] and, most frequently, a square-well potential [5].

Among the phenomena that arise in the photoionization of endohedral atoms, confinement resonances are of particular interest. They originate from the interference between photoionized electrons that are directly emitted from an ionized nl subshell and those photoionized electrons reflected from both the inner and outer boundaries of the fullerene cage.

The time-dependent close-coupling (TDCC) method [6] has been utilized in a series of studies [7–9] of the photoionization of endohedral atoms. These studies made use of a square-well model potential to represent the fullerene shell. Confinement resonance structure is predicted to be present in both the double-photoionization cross section [7] and the single-photoionization-with-excitation cross section [9].

A question arises as to the sensitivity of predicted phenomena to the form of the model potential used to represent the fullerene. In the model potential approach the width and radius of the potential is matched to available experimental data for the C_{60} shell, with the potential depth then adjusted to match the electron affinity of C_{60}. In this paper, the experimental work of Xu *et al.* [10] is used, which gives a potential width of 1.89 a.u. This width has been commonly adopted in the model potential approach to the photoionization of endofullerenes. However, we note that the photoelectron spectroscopy experiment of Rüdel *et al.* [11] indicates a larger C_{60} width of $\sim$3 a.u. A recent study [12] has also found indications of a 3-a.u. width in the experiment of Kilcoyne *et al.* [2]. The sensitivity to the depth and width of the confining potential was investigated for double photoionization in [8]. It was found that as the confining potential becomes wider and shallower (while maintaining the same electron affinity), the confinement resonances are decreased in amplitude. This can be attributed to a lowering in the reflective strength for scattered electrons as the potential depth is decreased [13]. Damping effects due to the representation of the confining potential was also studied in [14] for single photoionization, where an additional damping effect due to off-center positioning of the caged atom was examined.

A separate question concerns the approximation made as to the square-well form of the confining potential. It is of interest to relax the discontinuous nature of the potential. This has recently been investigated [15] for the single photoionization of H@C_{60} and Xe@C_{60} using a diffuse model potential formed from a combination of two Woods-Saxon potentials. This study found that the single-photoionization cross section is relatively insensitive to the degree of diffuseness, with good agreement found between results obtained using square-well and diffuse potentials. However, Ref. [16], which examined the single photoionization of H@C_{60}, Li@C_{60}, and Na@C_{60} using power-exponential potentials to model a diffuse C_{60} potential, found that the amplitude of confinement resonances was reduced.

It is of interest to investigate whether the double-photoionization cross section displays sensitivity to the diffuseness of the confining potential. Here, the TDCC method is used to study the single photoionization with excitation and the double photoionization of He@C_{60} using a diffuse potential to model the confining C_{60} shell.

The rest of this paper is structured as follows: Section II gives an overview of the TDCC calculations, and Sec. III presents results for the single photoionization with excitation and the double photoionization of He@C_{60} for square-well and diffuse confining potentials. Finally, Sec. IV concludes

*tgl0002@auburn.edu
†Present address: AquaQ Analytics, Forsyth House, Cromac Square, Belfast BT28LA, United Kingdom.

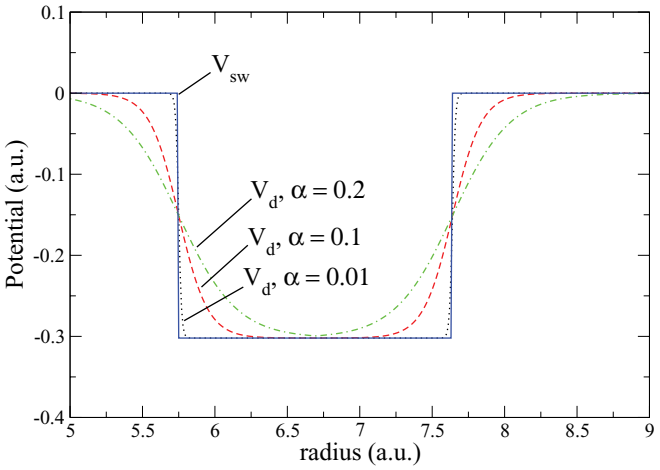

FIG. 1. (Color online) Model potentials. Solid line, square-well potential; dotted line, diffuse potential with $\alpha = 0.01$; dashed line, diffuse potential with $\alpha = 0.1$; dot-dashed line, diffuse potential with $\alpha = 0.2$.

with a brief summary. Unless otherwise stated, we will use atomic units throughout.

II. COMPUTATIONAL DETAILS

In order to represent a He atom enclosed within a C_{60} cage, an attractive, short-range spherical-shell potential will be used to approximate the fullerene shell. Two forms of this potential will be compared here. The first is a square-well potential of the form [5]

$$V_{sq}(r) = \begin{cases} -U_0 < 0 & \text{for} \quad r_c \leqslant r \leqslant r_c + \Delta, \\ 0 & \text{otherwise}, \end{cases} \tag{1}$$

where r_c is the inner radius of the shell and Δ is the shell thickness. The second is a diffuse potential formed from a linear combination of Woods-Saxon potentials [15],

$$V_d = -\left.\frac{U_0}{1+\exp\left(\frac{r_c - r}{\alpha}\right)}\right|_{r \leqslant r_c + \frac{\Delta}{2}} - \left.\frac{U_0}{1+\exp\left(\frac{r - r_c - \Delta}{\alpha}\right)}\right|_{r > r_c + \frac{\Delta}{2}}. \tag{2}$$

The square-well potential of Eq. (1) is compared to the diffuse potential given by Eq. (2) in Fig. 1 for varying levels of diffuseness. For $\alpha = 0.01$ the diffuse potential is very close to the square-well potential. As the diffuseness is increased to $\alpha = 0.1$ and $\alpha = 0.2$, the discontinuous boundary of the square-well potential becomes increasingly softened.

Values of the inner radius and shell thickness of C_{60} are determined from the experimental work of Xu *et al.* [10], with $r_c = 5.75$ and $\Delta = 1.89$ a.u. Diagonalizing on a radial mesh for an electron moving in the field $V_{sq}(r)$ with a potential depth of $U_0 = 8.22$ eV (0.302 a.u.) [17] leads to a calculated electron affinity of 2.66 eV. For the diffuse potential, diagonalizing for an electron moving in the field V_d with $\alpha = 0.01$ gives an electron affinity of 2.66 eV, in agreement with the square-well result. As α is increased to 0.1, the electron affinity is decreased to 2.59 eV, and for $\alpha = 0.2$ it is further decreased to 2.49 eV. These results compare to an experimentally measured electron affinity of 2.65 ± 0.05 eV [18]. It is noted that the recent investigation of [15] made use of a potential width and depth of $\Delta = 1.25$ a.u. and $U_0 = 11.48$ eV (0.422 a.u.) as these parameters were found [19] to lead to better agreement with experimental measurements for the $4d$ photoionization spectrum of $Xe@C_{60}^+$ [2]. Therefore, additional calculations are also carried out here at selected energy points for a deeper, narrower well of depth 11.0 eV (0.404 a.u.) and width $\Delta = 1.387$ a.u. for $\alpha = 0.01$ and $\alpha = 0.2$. The reduced width is needed in order to maintain the correct electron affinity.

The time-dependent Schrödinger equation in the weak-field limit for a two-electron atom enclosed by the model potential of Eq. (1) or (2) is given by

$$i\frac{\partial \Psi^{1P}(\vec{r}_1,\vec{r}_2,t)}{\partial t} = H_{\mathrm{He@C_{60}}}\Psi^{1P}(\vec{r}_1,\vec{r}_2,t) + H_{\mathrm{rad}}\Psi_0^{1S}(\vec{r}_1,\vec{r}_2)e^{-iE_0t}, \tag{3}$$

where

$$H_{\mathrm{He@}C_{60}} = \sum_i^2 \left[-\frac{1}{2}\nabla_i^2 + V(r_i) + V_{sq/d}(r_i)\right] + \frac{1}{|\vec{r}_1 - \vec{r}_2|} \tag{4}$$

and $V(r) = -\frac{2}{r}$ for the He atom. For a linearly polarized radiation field in the length gauge

$$H_{\mathrm{rad}} = E(t)\cos\omega t(r_1\cos\theta_1 + r_2\cos\theta_2), \tag{5}$$

where ω is the radiation field frequency and $E(t)$ is the radiation field amplitude.

The ground-state wave function for the He atom in the C_{60} cage, $\Psi_0^{1S}(\vec{r}_1,\vec{r}_2)$, and the energy E_0 are determined from an expansion in coupled spherical harmonics together with a relaxation of the time-dependent Schrödinger equation in imaginary time ($\tau = it$) [20,21].

Expansion of the time-dependent wave function $\Psi^{1P}(\vec{r}_1,\vec{r}_2,t)$ in coupled spherical harmonics and substitution into the time-dependent Schrödinger equation results in a set of time-dependent partial differential equations. These equations are then propagated in real time for 15 radiation field periods on a two-dimensional radial lattice with a mesh spacing of $\Delta r = 0.1$ and a lattice size of 640×640 points. The final time wave function is projected onto products of single-particle continuum orbitals to yield scattering probability amplitudes,

$$P_{l_1l_2}^{1P}(k_1,k_2,t) = \int_0^\infty dr_1 \int_0^\infty dr_2 P_{k_1l_1}(r_1)P_{k_2l_2}(r_2)P_{l_1l_2}^{1P}(r_1,r_2,t), \tag{6}$$

where $P_{l_1l_2}^{1P}(r_1,r_2,t)$ are radial wave functions for each l_1l_2 channel and box normalized continuum orbitals $P_{kl}(r)$ are calculated in a V^{N-2} potential in the presence of the fullerene cage using a uniform 1000-point momentum mesh with a mesh spacing of 0.002.

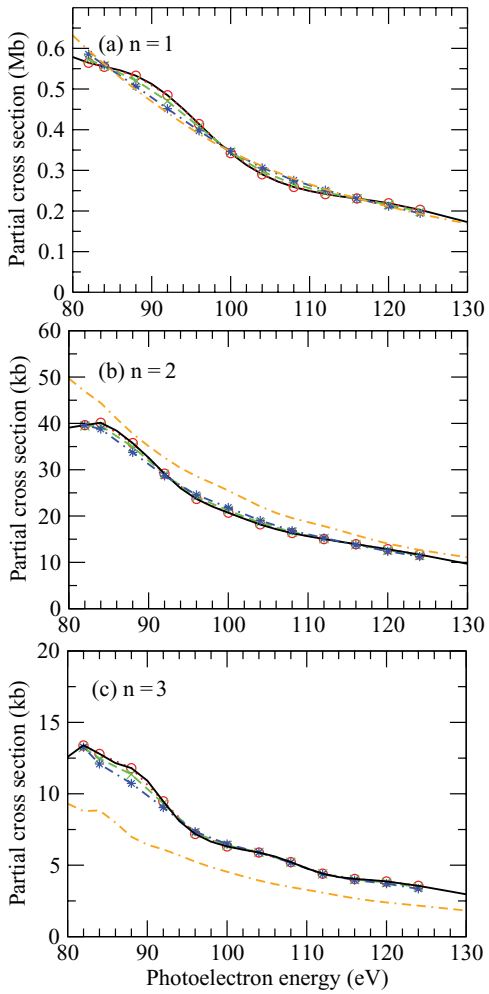

FIG. 2. (Color online) Single photoionization with excitation cross sections: (a) $n = 1$, (b) $n = 2$, (c) $n = 3$. Solid line, He@C_{60} with square-well potential; dotted line, He@C_{60} with diffuse potential ($\alpha = 0.01$); dashed line, He@C_{60} with diffuse potential ($\alpha = 0.1$); dot-dashed line, He@C_{60} with diffuse potential ($\alpha = 0.2$); dot-dash-dashed line, He.

The single-photoionization cross section with excitation to a bound state nl is then given by [22]

$$\sigma_{nl} = \frac{\omega}{I}\frac{\partial}{\partial t}\sum_{l_1,l_2}\left\{\int_0^\infty dk_2\left|\int_0^\infty dr_1\int_0^\infty dr_2 P_{nl}(r_1)P_{k_2l_2}(r_2)\right.\right.$$
$$\times P^{^1P}_{l_1l_2}(r_1,r_2,t)\Big|^2 + \int_0^\infty dk_1\left|\int_0^\infty dr_1\int_0^\infty dr_2 P_{k_1l_1}(r_1)\right.$$
$$\left.\left.\times P_{nl}(r_2)P^{^1P}_{l_1l_2}(r_1,r_2,t)\right|^2\right\}, \quad (7)$$

where $P_{nl}(r)$ is the radial orbital for the nl bound state of He@C_{60}. The total double-photoionization cross section can be calculated via the expression [23]

$$\sigma_{\rm dion} = \frac{\omega}{I}\frac{\partial}{\partial t}\int_0^\infty dk_1\int_0^\infty dk_2\sum_{l_1,l_2}\left|P^{^1P}_{l_1l_2}(k_1,k_2,t)\right|^2, \quad (8)$$

where I is the radiation field intensity.

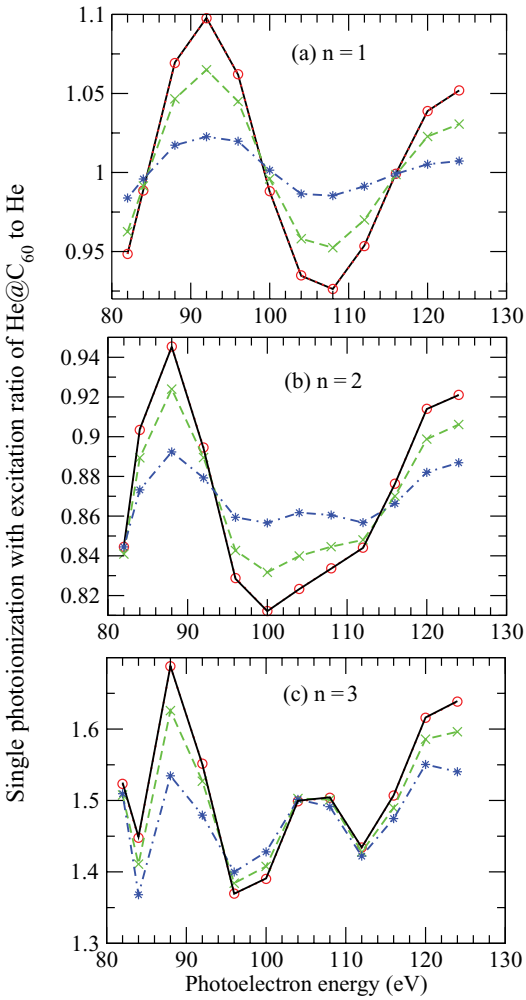

FIG. 3. (Color online) Ratio of single photoionization with excitation cross section of He@C_{60} to He: (a) $n = 1$, (b) $n = 2$, (c) $n = 3$. Solid line, He@C_{60} with square-well potential; dotted line, He@C_{60} with diffuse potential ($\alpha = 0.01$); dashed line, He@C_{60} with diffuse potential ($\alpha = 0.1$); dot-dashed line, He@C_{60} with diffuse potential ($\alpha = 0.2$).

III. RESULTS

In Fig. 2, the single-photoionization-with-excitation cross section of He@C_{60}, with the remaining He^+ ion left in excited states $n = 1$, $n = 2$, and $n = 3$ is plotted for the square-well potential of Eq. (1) and the diffuse potential of Eq. (2) with $\alpha = 0.01$, $\alpha = 0.1$, and $\alpha = 0.2$ in comparison with the cross section for He. Figure 3 shows the corresponding ratios of He@C_{60} to He for the cross sections in Fig. 2. The results for the square-well potential are in excellent agreement with the $\alpha = 0.01$ diffuse potential, showing that the diffuse potential with $\alpha \to 0$ is a good approximation to the discontinuous square-well potential. As the diffuseness of the potential is increased from $\alpha = 0.1$ to $\alpha = 0.2$, the confinement resonance structure seen in Fig. 3 is damped, with a decreasing amplitude. For $n = 1$, with increased damping the cross sections approach those of He. For $n = 2$ and $n = 3$ the cross sections are shifted in magnitude from those of He due to the stronger effect of the confining potential on these more radially extended excited states.

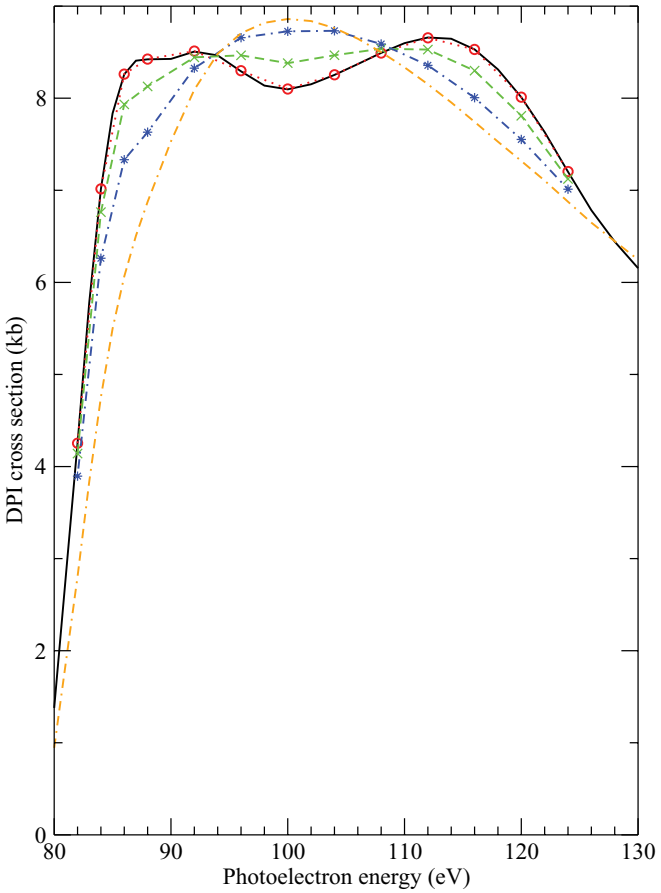

FIG. 4. (Color online) Double-photoionization cross sections. Solid line, He@C_{60} with square-well potential; dotted line, He@C_{60} with diffuse potential ($\alpha = 0.01$); dashed line, He@C_{60} with diffuse potential ($\alpha = 0.1$); dot-dashed line, He@C_{60} with diffuse potential ($\alpha = 0.2$); dot-dash-dashed line, He.

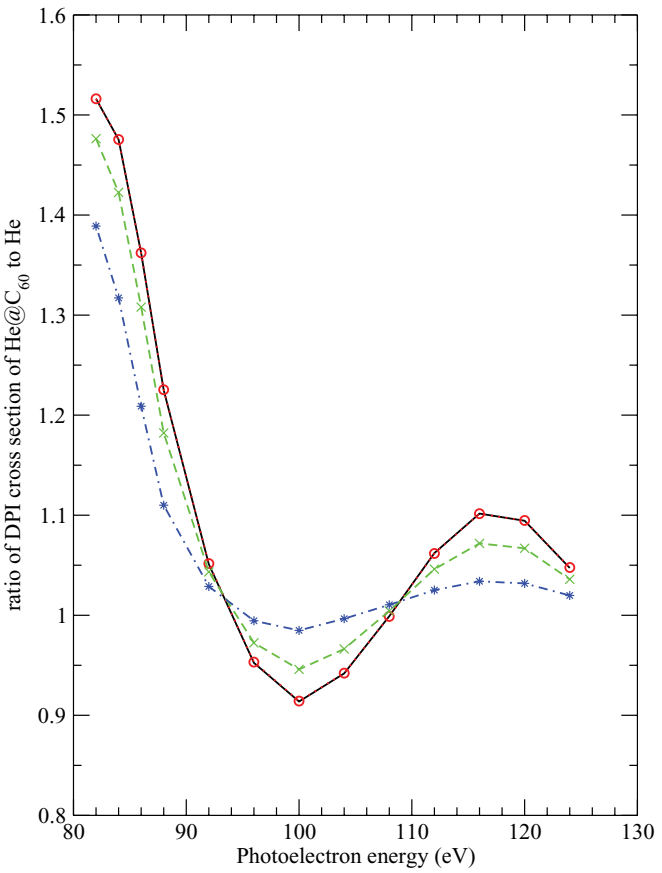

FIG. 5. (Color online) Ratio of double-photoionization cross section of He@C_{60} to He. Solid line, He@C_{60} with square-well potential; dotted line, He@C_{60} with diffuse potential ($\alpha = 0.01$); dashed line, He@C_{60} with diffuse potential ($\alpha = 0.1$); dot-dashed line, He@C_{60} with diffuse potential ($\alpha = 0.2$).

Figure 4 shows the double-photoionization cross section of He@C_{60} for the square-well potential of Eq. (1) and the diffuse potential of Eq. (2) with $\alpha = 0.01$, $\alpha = 0.1$, and $\alpha = 0.2$ in comparison with the cross section for He. Figure 5 shows the corresponding ratios of He@C_{60} to He for the cross sections in Fig. 4. As with the cross sections for single photoionization with excitation, the double photoionization cross sections for the square-well potential and the diffuse potential with $\alpha = 0.01$ agree closely with each other. The results for $\alpha = 0.1$ and $\alpha = 0.2$ show damping of confinement resonances, with the ratios plotted in Fig. 5 approaching 1 for higher energies and higher diffuseness of the potential. However, at lower energies, there is still a large deviation from the isolated He results for $\alpha = 0.2$. Unlike the damping effect illustrated in [8], where the amplitude of the confinement oscillations decreased as the confining potential was made shallower and wider, here there is no phase shift in the locations of the peaks of the confinement resonances, showing that this is a distinct effect.

This damping effect caused by the diffuseness of the potential is seemingly in conflict with the insensitivity found for single photoionization in [15]. To investigate this discrepancy, additional calculations were carried out at 86, 100, and 116 eV for $\alpha = 0.01$ and $\alpha = 0.2$ using a deeper well of depth 0.404 a.u. and width $\Delta = 1.387$ a.u. The results are tabulated in Table I and show that the deeper well is insensitive to the diffuseness of the potential, with similar results found for $\alpha = 0.01$ and $\alpha = 0.2$. This can be explained by the weaker reflective strength of shallower potentials [13] leading to more sensitivity to diffuseness. The present results for double photoionization also demonstrate that the results of Ref. [16], where sensitivity to diffuseness was found in the single-photoionization cross section (see Figs. 7, 9, and 11 of [16]), can be caused by the shallower potential of $U_0 = 0.303$ a.u. as opposed to the deeper potential of $U_0 = 0.422$ a.u. used in [15].

TABLE I. Double-photoionization (DPI) cross section of He@C_{60} for $U_0 = 0.404$ a.u. and $\Delta = 1.387$ a.u.

Photon energy	DPI cross section (kb)		DPI ratio
(eV)	$\alpha = 0.01$	$\alpha = 0.2$	$\alpha = 0.2$ to $\alpha = 0.01$
86	8.82	8.32	0.94
100	9.44	9.35	0.99
116	7.99	8.06	1.01

IV. CONCLUSIONS

In this paper it has been demonstrated that both the single photoionization with excitation and the double photoionization of $He@C_{60}$ are sensitive to the diffuseness of the model potential. For shallower and wider potentials, the confinement resonance structure that is observed in calculations using commonly adopted model potential parameters is progressively damped as the diffuseness of the potential is increased. However, as the potential becomes deeper and narrower, the photoionization cross section becomes insensitive to the diffuseness of the potential.

To further investigate these effects, comparison with other theoretical methods, such as convergent close coupling [24] or R matrix with pseudostates [25], is highly desirable for the double photoionization of $He@C_{60}$. The recent R-matrix study of the single photoionization of $Xe@C_{60}$ [26] is a promising step in this direction.

ACKNOWLEDGMENTS

We wish to thank Tom Gorczyca for useful discussions and the referee for helpful comments. This work was supported in part by grants from the US Department of Energy. Computational work was carried out at the National Energy Research Scientific Computing Center in Oakland, California.

[1] V. K. Dolmatov, in *Theory of Confined Quantum Systems: Part Two*, Advances in Quantum Chemistry Vol. 58, edited by J. R. Sabin and E. Brändas (Academic, New York, 2009), pp. 13–68.
[2] A. L. D. Kilcoyne, A. Aguilar, A. Müller, S. Schippers, C. Cisneros, G. Alna'Washi, N. B. Aryal, K. K. Baral, D. A. Esteves, C. M. Thomas, and R. A. Phaneuf, Phys. Rev. Lett. **105**, 213001 (2010).
[3] H. S. Chakraborty, M. E. Madjet, J.-M. Rost, and S. T. Manson, Phys. Rev. A **78**, 013201 (2008).
[4] M. Y. Amusia, A. S. Baltenkov, L. V. Chernysheva, Z. Felfi, and A. Z. Msezane, J. Phys. B **38**, L169 (2005).
[5] J. P. Connerade, V. K. Dolmatov, P. A. Lakshmi, and S. T. Manson, J. Phys. B **32**, L239 (1999).
[6] M. S. Pindzola *et al.*, J. Phys. B **40**, R39 (2007).
[7] J. A. Ludlow, T-G. Lee, and M. S. Pindzola, Phys. Rev. A **81**, 023407 (2010).
[8] J. A. Ludlow, T-G. Lee, and M. S. Pindzola, J. Phys. B **43**, 235202 (2010).
[9] T-G. Lee, J. A. Ludlow, and M. S. Pindzola, J. Phys. B **45**, 135202 (2012).
[10] Y. B. Xu, M. Q. Tan, and U. Becker, Phys. Rev. Lett. **76**, 3538 (1996).
[11] A. Rüdel, R. Hentges, U. Becker, H. S. Chakraborty, M. E. Madjet, and J. M. Rost, Phys. Rev. Lett. **89**, 125503 (2002).
[12] A. B. Patel and H. S. Chakraborty, J. Phys. B **44**, 191001 (2011).
[13] M. A. McCune, M. E. Madjet, and H. S. Chakraborty, Phys. Rev. A **80**, 011201(R) (2009).
[14] A. S. Baltenkov, U. Becker, S. T. Manson, and A. Z. Msezane, J. Phys. B **43**, 115102 (2010).
[15] V. K. Dolmatov, J. L. King, and J. C. Oglesby, J. Phys. B **45**, 105102 (2012).
[16] C. Y. Lin and Y. K. Ho, J. Phys. B **45**, 145001 (2012).
[17] V. K. Dolmatov and S. T. Manson, Phys. Rev. A **73**, 013201 (2006).
[18] L. S. Wang, J. Conceicao, C. Jin, and R. E. Smalley, Chem. Phys. Lett. **182**, 5 (1991).
[19] V. K. Dolmatov and D. A. Keating, J. Phys. Conf. Ser. **388**, 022097 (2012).
[20] M. S. Pindzola and F. Robicheaux, Phys. Rev. A **57**, 318 (1998).
[21] D. M. Mitnik, J. Randazzo, and G. Gasaneo, Phys. Rev. A **78**, 062501 (2008).
[22] J. Colgan and M. S. Pindzola, Phys. Rev. A **67**, 012711 (2003).
[23] J. Colgan, M. S. Pindzola, and F. Robicheaux, J. Phys. B **34**, L457 (2001).
[24] A. S. Kheifets and I. Bray, Phys. Rev. A **54**, R995 (1996).
[25] T. W. Gorczyca and N. R. Badnell, J. Phys. B **30**, 3897 (1997).
[26] T. W. Gorczyca, M. F. Hasoglu, and S. T. Manson, Phys. Rev. A **86**, 033204 (2012).